A Nulling Widen and Deepening Algorithm using a Modified Correlation Subtraction Algorithm Multistage Wiener Filtering

Xiao Li and Xinhuai Wang

Department of Electrical Engineering
Xidian University, Xian 710071, China
hxazgsja075@gmail.com

Abstract **–** The calculation of beamforming weights takes time due to the constantly changing direction of interference in highly dynamic environments. The traditional anti-jamming means under static or low dynamic are almost all invalid, so the nulling widen algorithm is studied. However, the commonly used cavitation widening and deepening algorithms are often accompanied by a large amount of computational complexity, which may lead to computational inefficiency and slow processing speed in practical applications. In order to solve this problem, a nulling widen and deepening algorithm using a modified correlation subtraction algorithm multistage Wiener filtering is proposed. The algorithm achieves the deepening after nulling widening by constructing a new covariance matrix, and then reduces the rank by truncating the multilevel Wiener filter at the r-level. It finds the blocking matrix with the normalized reference vectors instead of calculating the blocking matrix directly so that the normalized reference vectors are orthogonal to each other, and finally completes the interference suppression by using the power inversion algorithm to improve the performance and reduce the amount of computation. The computational complexity of the algorithm based on the modified correlation subtraction algorithm multistage Wiener filtering (MCSA-MWF) is $O\left(rM^2\right)$, which is greatly reduced compared to the computational complexity of the traditional null-spread class algorithm with direct inversion $O\left(M^3\right)$.

Index Terms **–** Adaptive anti-jamming, modified correlation subtraction algorithm multistage Wiener filtering (MCSA-MWF), nulling widen and deepening.

I. INTRODUCTION

Satellite navigation technology provides users with coordinates in time and space, which is of great strategic military importance in aviation, space and guided weapons, as well as being of great economic interest, and is nowadays indispensable in the transport industry. Satellite navigation technology is in great demand both in the military and civilian sectors.

Since the satellite is very far away from the receiver and the transmit power of the satellite is very weak, the navigation signal is very likely to receive interference [1, 2]. However, under high dynamic conditions, traditional anti-jamming means under static or low dynamic are almost all invalid, so the nulling widen algorithm is studied.

The nulling technique forms a stable beam nulling in the direction of the interference to provide cancellation with the interfering signal. The nulling widen algorithms are generally divided into interference-plus-noise covariance (INC) and the nulling widen algorithms based on covariance matrix taper (CMT) [4]. INC algorithms are generally more computationally intensive and often require some a priori information such as the direction of the interference and the direction of the desired signal [5]. In cases where the incoming information of the desired signal is known, the nulling is widened by removing the expected signal from the covariance matrix. In contrast, the CMT algorithm is much less computationally intensive. The CMT algorithm was proposed by Mailloux [4], which rewrites the covariance matrix by setting up a virtual interference to widen the nulling with a taper matrix.

Other scholars have proposed different methods for nulling widen. Zatman [7] converts the narrowband interference signal into a virtual broadband interference signal to widen the nulling. Li et al. [8] established a Gaussian distribution model based on the interference. Based on the Gaussian distribution, Cong et al. [9] designed an algorithm to deepen the nulling by perspective drawing. Zeng et al. [10] theoretically deduced that the sufficient condition for the FIR filter not to change the zero value is the symmetry of coefficients or conjugate symmetry. On this basis, a nulling widen algorithm based on virtual interference is proposed [11]. A new method of space-time joint adaptive processing (STAP) null-widen is deduced based on the Laplace distribution model of the changing interference direction of arrival (DOA) in a high-dynamic environment [12, 13] by taking the moving interferences as discrete interference sources

Submitted On: April 28, 2024
Accepted On: September 29, 2024

1054-4887 © ACES

https://doi.org/10.13052/2024.ACES.J.390807

that obey the Laplace distribution. Thus, the average covariance matrix can be calculated to broaden the width of nulls. In [22], a procedure for the null widen algorithm design with respect to the nonstationary interference is proposed.

In addition, many more studies have focused on covariance matrices. For nulling widen, [14] is implemented by a simple modification of the measured covariance matrix. Reference [15] explores the theory and application of covariance matrix tapers for robust adaptive beamforming. In [16], CMTs and derivative constraints in the directions of jammers have been proposed to widen the nulling in adaptive processing, thereby improving the algorithms' robustness. Reference [17] develops a computationally efficient online implementation of the CMT technique based on a low-rank approximation of the taper matrix and the recursive least squares (RLS) algorithm. In reference [18], by means of the covariance matrix of the auxiliary elements, a nulling widen method was realized based on the sidelobe canceller. This approach demonstrated good performance in practical applications, but has increased hardware complexity. Reference [23] proposed a computationally efficient nulling widen method for sidelobe canceller, which is a CMT based method and puts fictitious interference into snapshots to broaden the sharp null. Based on Mailloux's methodology, the covariance matrix and cross-correlation vector were tapered via random disturbance. Compared with the existing methods, the method required much less computation, but its performance is similar.

Meanwhile, some studies have reconstructed the algorithmic correlation matrix (such as INC matrix and covariance matrix) to achieve nulling widen. In [19, 20], an adaptive null widen technique based on reconstruction of the covariance matrix was proposed. Reference [21] proposes an algorithm based on INC matrix reconstruction by setting up several virtual interference sources, which can simultaneously broaden the nulls. Null depth and width can be controlled by setting the parameters of the virtual interference sources.

The multistage Wiener filter (MWF) [24] is a multilevel equivalent realization of the Wiener filter, which uses a sequence of orthogonal projections to decompose the array signal vectors at multiple levels, and then performs multistage scalar Wiener filtering to synthesize the error signals of the Wiener filter. Depending on the blocking matrix, the multilevel Wiener filter can be implemented with different algorithms. The MWF was first proposed by Goldstein, Reed, and Scharf in [24], whose Appendix A gives a method for calculating the blocking matrix, and calls the algorithm GRS-MWF, with GRS being an abbreviation of the authors' names. References [25–28] proposed a MWF implementation method that effectively reduces the computational effort called the correlation subtraction algorithm, denoted CSA-MWF. Reference [29] proposed a modified correlation subtraction algorithm multistage Wiener filtering (MCSA-MWF) based on CSA algorithm, which improves the blocking matrix of CSA-MWF so as to have the advantages of GRS-MWF. The improved blocking matrix can be realized with the CSA structure. This results in good numerical stability, i.e., reduced-rank performance, and a further reduction in computational effort.

In order to reduce the amount of computation and make it more robust even in small snapshot environments, we combined the MCSA-MWF with the CMT algorithm to propose a nulling widen and deepening algorithm using a modified correlation subtraction algorithm MWF.

The main contributions of this paper are as follows:

A new MCAS-MWF based nulling widen and deepening algorithm is proposed, which can improve the stability of the algorithm for small snapshot data in highly dynamic environments.

The normalized reference vectors are used to solve for the blocking matrix instead of computing (constructing) the blocking matrix, thus making the normalized reference vectors orthogonal to each other and effectively reducing the arithmetic.

We compare the performance of the MCAS-MWF based nulling widen and deepening algorithm through typical experiments. The simulation experiments show that the proposed algorithm has good performance under both ideal circular array conditions and real measured BeiDou data.

The rest of the paper is organized as follows: section II introduces the signal model, section III describes the nulling spread-and-deepen algorithm based on MCAS-MWF, section IV demonstrates the simulation of the algorithm under the ideal uniform circular array and the real measured BeiDou data, and section V concludes the work of this paper.

II. SIGNAL MODELLING

A. Arbitrary plane array system model

As is shown in [32], for a two-dimensional M-element arbitrary array planar array, in the setting of L signal, Q interference, the received data model of the signal in an environment with four interferences is:

$$X(t) = X_S(t) + X_I(t) + n \tag{1}$$
$$= \sum_{I=1}^{L} a(\theta_1, \varphi_1) s_1(t) + \sum_{q=1}^{Q} a(\theta_q, \varphi_q) s_q(t) + n,$$

where $X_S(t)$ is the received desired signal source, $X_1(t)$ is the interference signal received and n is the noise. (θ_1, φ_1) and (θ_q, φ_q) are the incoming direction of the

$1th$ signal and the qth interference, respectively. θ and φ are the pitch and azimuth angles. $s_1(t)$ and $s_q(t)$ are the $1th$ signal and the qth interference, respectively. a is the airspace guidance vector. For any 2D planar array, the airspace guidance vector is:

$$a(\theta,\varphi)=\left[e^{juT(\theta,\varphi)P_1},e^{juT(\theta,\varphi)P_2},e^{juT(\theta,\varphi)P_m}\right], \quad (2)$$

where P_m is the position vector of the mth array element and u is the beam vector with the expression:

$$P_m=d_m[\cos r_m,\sin r_m]^T, \quad (3)$$

$$u(\theta,\varphi)=\frac{2\pi}{\lambda}\begin{bmatrix}\sin(\theta)\ \cos(\varphi)\\ \sin(\theta)\ \sin(\varphi)\end{bmatrix}. \quad (4)$$

$\pi=3.14$, $\lambda\in(380\sim760)nm$, d_m expressed as $d_m=\sqrt{x_m^2+y_m^2}$, i.e., the Euclidean distance of each array element from the reference array element. r_m is the angle of each array element.

The power inversion algorithm (PI) is used for the anti-interference process and its weights are calculated as follows:

$$w_{opt}=\left(s^HR^{-1}s\right)^{-1}R^{-1}s, \quad (5)$$

where s is the constraint vectors and, at the same time, $s=[1,0,...,0]^T$. R is the covariance matrix of the received signal. The superscript$\{\cdot\}^H$ denotes the Emmett transpose. The sampled data is used in practical engineering to approximate R:

$$\tilde{R}=\frac{1}{K}\sum_{k=1}^{K}X(k)X^H(k), \quad (6)$$

where K is the number of sampling beats and $\tilde{R}\to R$ when $K\to\infty$.

B. BeiDou signal model

The BeiDou Navigation Satellite System (BDS) launched the construction of the BeiDou Satellite Navigation Pilot System in 1994, completed the BeiDou II regional service system in 2012, and completed the full-scale construction of the BeiDou III system in 2020, achieving the goal of global navigation and positioning.

According to the B3I interface control document [30], the expression for the B3I signal is:

$$S_{B3I}^j(t)=A_{B3I}C_{B3I}^j(t)D_{B3I}^j(t)\cos\left(2\pi f_3t+\varphi_{B3I}^j\right), \quad (7)$$

where A_{B3I} denotes the amplitude of the B3I signal, C_{B3I}^j denotes the ranging code of satellite j, D_{B3I}^j denotes the data code of satellite j, f_3 denotes the carrier frequency of the B3I signal, and the nominal carrier frequency is 1268.52 MHz. φ_{B3I} denotes the signal carrier initial phase and the bandwidth of the B3I signal is 20.46 MHz.

The generation mechanism of the BeiDou signal is shown in Fig. 1. One pseudo-random code cycle is modulo two-added to one NH code bit, and one NH code cycle is modulo two-added to one navigation message bit, followed by BPSK modulation to produce the space RF signal. Each satellite has a unique ranging code, and

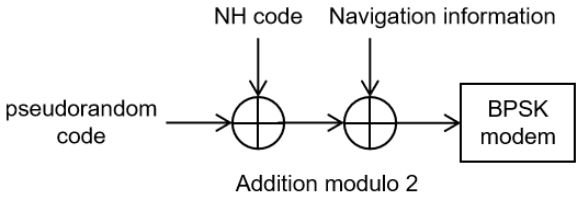

Fig. 1. Schematic diagram of BeiDou B3I signal coding process.

the ranging code CB3I for B3I has a code rate of 10.23 Mcps and a period of 10230.

III. MCAS-MWF BASED NULLING WIDENING AND DEEPENING ALGORITHM

A. Principle of nulling widening and deepening algorithm

Since the direction of interference in high-speed environments changes constantly, the calculation of beamforming weights takes time, and the calculated weights are strictly applicable to the moment before the calculation of the weights. Thus, the direction of interference will change rapidly. Moreover, the width of the conventional beamforming nulling is particularly narrow, so once the direction of interference changes slightly, it will be out of the generated nulling area, and the nulling will not allow the interference to come in and generate an offset. Thus, the effect of interference suppression will be rapidly degraded, which makes the anti-jamming algorithm ineffective. In order to keep the anti-jamming algorithm stable in the high-speed environment, the commonly used algorithm is the nulling widen algorithm.

Nulling widen is achieved using the CMT method. The effect of change in the direction of the interference is embodied in the covariance matrix R of the received signal, under the action of the taper matrix T.

For a nulling spread of a line matrix [8], the taper matrix T is:

$$T_{k,l}=e^{\left\{\frac{1}{2\sigma_{\max}^2[(k-1)\pi/180]^2}\right\}}, \quad (8)$$

where $\sigma_{\max}^2$ determines the width of the nulling. The new covariance matrix $\bar{R}$ is obtained from the Hadamard product of the taper matrix $T_{k,l}$ and the old covariance matrix R. The conical covariance matrix is:

$$\bar{R}_L=\tilde{R}^{\circ}\bar{T}_L. \quad (9)$$

Nulling widen can be produced by solving for the beamforming weights using the tapered covariance matrix. In order to achieve nulling widen and deepening on this basis, the sampled covariance matrix of equation (6) is eigen-decomposed:

$$\tilde{R}=\sum_{m=1}^{M}\lambda_m e_m e_m^H, \quad (10)$$

where λ_m is the eigenvalue of $\tilde{R}$, e_m is the corresponding eigenvector. λ_m in descending order, and its magnitude, reflects the power of the corresponding signal or interference:

$$\lambda_1 \geq \lambda_2 \cdots \geq \lambda_Q > \lambda_{Q+1} = \cdots = \lambda_M = \sigma_n^2. \quad (11)$$

In the navigation receiver the interference energy is much larger than the navigation signal, so the first Q large eigenvalues correspond to the subspace of the interference, so that the set is $U_I = [e_1, e_2, \cdots, e_Q]$. The equation is as follows:

$$\begin{aligned} &span\{a(\theta_1,\phi_1), a(\theta_2,\phi_2), \cdots, a(\theta_Q,\phi_Q)\} \\ &\quad = span\{e_1, e_2, \cdots, e_Q\} \end{aligned}. \quad (12)$$

Afterwards, a projection transformation is performed to extract the interference components and then weight the coefficients of the interference components to obtain the processed sampled data as:

$$\bar{X}(k) = X(k) + gTX(k) = (I_k + gT)X(t). \quad (13)$$

Based on the characteristic subspace property, the projection matrix of the interference subspace is found to be:

$$T = U_I \left(U_I^H U_I\right)^{-1} U_I^H, \quad (14)$$

where g is a weighting factor that serves to change the nulling depth in dB, U_I is signal subspace.

Finally, the new covariance matrix after preprocessing is:

$$\begin{aligned} \tilde{R}_T &= \frac{1}{K}\sum_{k=1}^{K} \bar{X}(k)\bar{X}^H(k) \\ &= (I_K + gT)\tilde{R}(I_K + gT)^H, \end{aligned} \quad (15)$$

where $\tilde{R}_T$is the covariance matrix after taper, I_K is a unit matrix of length K. This covariance matrix is used to replace the previous sampling covariance matrix.

B. Correlated phase reduction MWF

MWF [31] is an equivalent algorithm to the Wiener filter, which avoids matrix inversion and thus reduces the volume of computation. Correlation subtraction algorithm multistage Wiener filtering (CSA-MWF) further reduces the forward recursion based on MWF and avoids blocking matrix computation compared to MWF. MCSA-MWF further reduces the number of dimensions, and its block diagram is shown in Fig. 2. In GRS-MWF, its blocking matrix uses the $(N-i-1)\times(N-i)$ rectangular matrix B_i, and the dimension of $X(k)$ decreases step by step, which is conducive to reducing the computation and storage. CSA-MWF is a Wiener multistage filter with subspace basis vectors orthogonal to each other, the blocking matrices B_i are all N-dimensional square matrices, and all levels of observation data $X_i(k)$ are also N-dimensional square matrices. From the principle of CSA-MWF, it can be seen that reduced-rank processing does not lead to the reduction of dimension, so the data redundancy is large. It can be envisioned that if the blocking matrix is adopted as a $(N-i-1)\times(N-i)$ rectangular matrix, it not only utilizes the CSA structure of CSA-MWF without solving the blocking matrix, but also exploits the advantages of GRS-MWF's dimension reduction, making the $X_i(k)$ dimension of the MWF reduce step by step. This structure is referred to as MCSA-MWF, and the structure is shown in Fig. 2 [31], which combines the advantages of GRS-MWF and CSA-MWF to obtain almost the same performance as CSA-MWF, but with less computational effort than both.

In Fig. 2, the forward recursive formula for MCSA-MWF level i is as follows:

$$h_i = \frac{r_{X_{i-1}d_{i-1}}}{\sqrt{r_{X_{i-1}d_{i-1}}^H r_{X_{i-1}d_{i-1}}}}, \quad (16)$$

$$d_i(k) = h_i^H X_{i-1}(k), \quad (17)$$

$$B_i = I_{N-i}^{(N-i-1)} - h_i^{(N-i-1)} h_i^H, \quad (18)$$

$$X_i(k) = B_i X_{i-1}(k) = X_{i-1}^{(N-i-1)}(k) - h_i^{(N-i-1)} d_i(k), \quad (19)$$

where h_i is N-dimensional, $X_i(k)$ is an $N-i-1$ dimensional vector, and $I_{N-i}^{(N-i-1)}$ denotes the upper $N-1$ rows of the N-dimensional unit array.

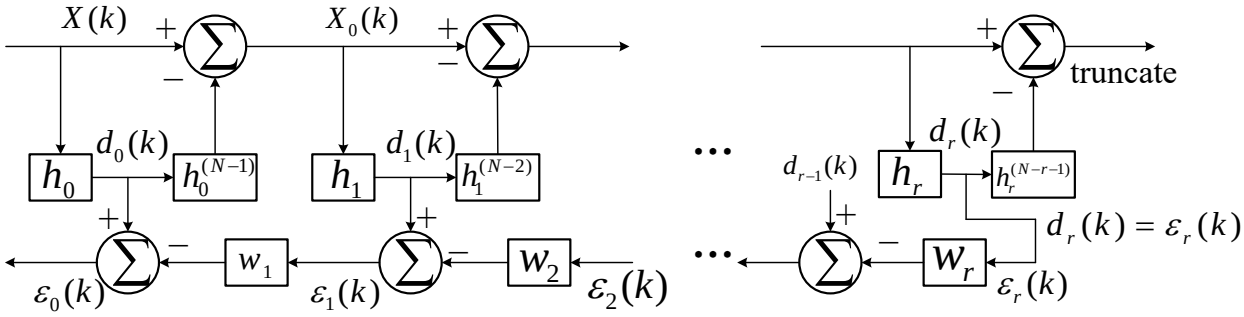

Fig. 2. MCSA-MWF structure block diagram.

C. An MCAS-MWF based nulling widen and deepening algorithm

According to [6], the MCSA-MWF weights are solved for:

$$W_{MCSA-MWF} = h_0 - B_0^H T_D W_d. \tag{20}$$

When using the power inversion algorithm:

$$h_0 = [1,0,\cdots,0]^T, \tag{21}$$

$$T_D = [t_1, t_2, \cdots, t_D], \tag{22}$$

$$t_i = \left(\prod_{j=1}^{i-1} B_j^H\right) h_i, \tag{23}$$

$$h_i = \frac{r_{X_{i-1}d_{i-1}}}{\left\| r_{X_{i-1}d_{i-1}} \right\|}, \tag{24}$$

included among these:

$$r_{X_{i-1}d_{i-1}} = E\left[X_{i-1}d_{i-1}^*\right] \tag{25}$$

$$= B_{i-1}\left(\prod_{r=i-2}^{0} B_r\right) R_{XX} \left(\prod_{r=i-2}^{0} B_r\right)^H h_{i-1},$$

$$B_i = I_{M-i}^{(M-i-1)} - h_i^{(M-i-1)} h_i^H, \tag{26}$$

$$W_d = \left(T_D^H B_0 R_{XX} B_0^H T_D\right)^{-1} T_D^H B_0 R_{XX} h_0, \tag{27}$$

where r is the order of the truncated reduced rank, and $h_i i = 1,2,3...,D)$ is the recursive weights in the MWF, B_i is the blocking matrix, W_d is the backward Wiener filter, R_{XX} is the received signal autocorrelation matrix, and t_i is the basis vector of the reduced-rank subspace. Equation (26) can be obtained from [3], the superscript n of it denotes the upper n rows of the fetch matrix. After derivation, the weights of MCSA-MWF-PI can be calculated as:

$$W_{MCSA-MWF-PI} = h_0 - B_0^H T_D \left(T_D^H B_0 R_{XX} B_0^H T_D\right)^{-1} T_D^H B_0 R_{XX} h_0. \tag{28}$$

By bringing equation (9) of $\overline{\mathrm{R_L}}$ into the above equation, then the Laplace nulling widen power inversion algorithm based on the MCSA-MWF-LNW-PI is:

$$W_{MCSA-MWF-LNW-PI} = h_0 - B_0^H T_D \left(T_D^H B_0 \bar{R}_L B_0^H T_D\right)^{-1} T_D^H B_0 \bar{R}_L h_0. \tag{29}$$

By bringing equation (15) of $\widetilde{\mathrm{R}}_{\mathrm{T}}$ into the above equation, then the Laplace nulling widen and deepening power inversion algorithm based on the MCSA-MWF-LNWD-PI is:

$$W_{MCSA-MWF-LNWD-PI} = h_0 - B_0^H T_D \left(T_D^H B_0 \tilde{R}_T B_0^H T_D\right)^{-1} T_D^H B_0 \tilde{R}_T h_0. \tag{30}$$

As shown in the Table 1, compared with the computational complexity of the conventional nulling widen algorithm for direct inverse $\mathrm{O}\left(\mathrm{M}^3\right)$, the computational complexity of the algorithm based on the MCSA-MWF-LNWD-PI is $\mathrm{O}\left(\mathrm{rM}^2\right)$. If it is a N-tap null-time joint algorithm, the computational complexity of the algorithm changes from $\mathrm{O}\left((\mathrm{MN})^3\right)$ to $\mathrm{O}\left(\mathrm{r}(\mathrm{MN})^2\right)$, which greatly reduces the computational complexity.

Table 1: Comparison of the computational complexity of the two nulling widen algorithms

Arithmetic	Complexity	N-tap Null-Time Joint Algorithm
Conventional algorithm	$\mathrm{O}\left(\mathrm{M}^3\right)$	$\mathrm{O}\left((\mathrm{MN})^3\right)$
Based on the MCSA-MWF-LNWD-PI	$\mathrm{O}\left(\mathrm{rM}^2\right)$	$\mathrm{O}\left(\mathrm{r}(\mathrm{MN})^2\right)$

IV. ALGORITHM SIMULATION

In this section, we use the ideal seven-element uniform circular array and seven-channel measured BeiDou data to carry out algorithm simulation separately and compare the anti-jamming performance of different algorithms.

A. MCSA-MWF performance analysis

There are several different algorithmic implementations of the multilevel Wiener filter, such as CSA-MWF, GRS-MWF, and MCSA-MWF. In CSA-MWF, the blocking matrices B_i are all N-dimensional square matrices, and the observation data $X_i(k)$ at each level are all N-dimensional vectors. The blocking matrices of MCSA-MWF adopt the rectangular matrices of size $(N-i-1)\times(N-i)$, which can take advantage of the CSA structure of CSA-MWF, which does not need to solve the blocking matrices and reduces computation. An advantage of the decreasing dimension of $X_i(k)$ in GRS-MWF is to further reduce computation while maintaining the reduced-rank performance.

In adaptive beamforming based on the GSC framework, in addition to the usual performance metrics (e.g., array orientation map, output signal-to-noise ratio), there is also a special metric called mean square error (MSE). Several implementations of MSE are defined [29]:

$$MSE = W_X^H R W_X, \tag{31}$$

$$SMSE = W_X^H R_X W_X, \tag{32}$$

$$MMSE = W_{opt}^H R W_{opt}. \tag{33}$$

MSE is the result obtained by applying the sampled adaptive weight vector print to the ideal array data statistics. SMSE (sample mean square error) is the result obtained by applying the sampled adaptive weight vector to the training data itself. MMSE (minimum mean square error) is the result obtained by applying the ideal adaptive weight vector to the ideal array data statistics.

Now let us compare the three MWFs mentioned above using these metrics. Figure 3 shows the curve of MMSE with the rank change of three different algorithms in a uniform linear array with N=16 elements. Since MMSE examines the performance of the algorithm from the overall statistical characteristics, it can reflect the performance of the algorithm under certain signal

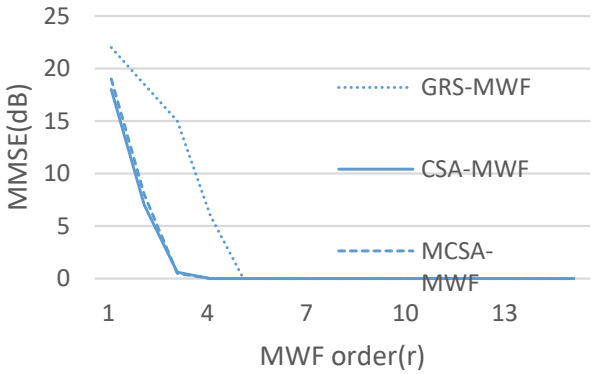

Fig. 3. The curve of MMSE with rank change of three different algorithms in a uniform linear array.

statistical characteristics. Thus, MMSE is an important indicator of the performance of the algorithm. In Fig. 3, the MMSE curve of MCSA-MWF and CSA-MWF are close to the minimum at r = 3.

Let the rank of the reduced-rank multilevel Wiener filter be r and the number of snapshots be K, then the computational amount (number of multiplications) of the three r-order multilevel Wiener filters GRS-MWF, CSA-MWF, MCSA-MWF can be compared as shown in Table 2, which refers to the computational amount of the forward recursion since the backward recursive synthesis is exactly the same. It can be seen that the computation amount of GRS-MWF is $O\left(N^2\right)$, while that of CSA-MWF and MCSA-MWF is only $O(N)$, and the number of multiplications of MCSA-MWF is lower than that of CSA-MWF by $Kr(r+1)$ times. It can be seen that MCSA-MWF is especially suitable for large arrays with more adaptive degrees of freedom, such as the spatial adaptive processing in complex interference environments. MCSA-MWF is finally used instead of CSA-MWF because the blocking matrix of MCSA-MWF is rectangular, which reduces the computational effort.

Table 2: Comparison of the computational complexity of the two nulling widen algorithms

Algorithm / Calculated amount	$X_i(k)=B_iX_{i-1}(k)$	$d_i(k)=h_i^HX_{i-1}(k)$
GRS-MWF	$K[N^2+(N-1)^2+...+(N-r+1)^2]$	$K[N+(N-1)+...+(N-r)]$
CSA-MWF	$KN(r)$	$KN(r+1)$
MCSA-MWF	$K[(N-1)+...+(N-r)]$	$K[N+(N-1)+...+(N-r)]$

Figures 4 and 5 show the relationship between the nulling angel/gain and the MWF order, demonstrating the orientation and gain at different ranks. The best results are obtained when r=6, the gain in this case did not disappear and is the minimum. Therefore, in later simulation experiments, we chose the rank of MCSA-MWF as 6.

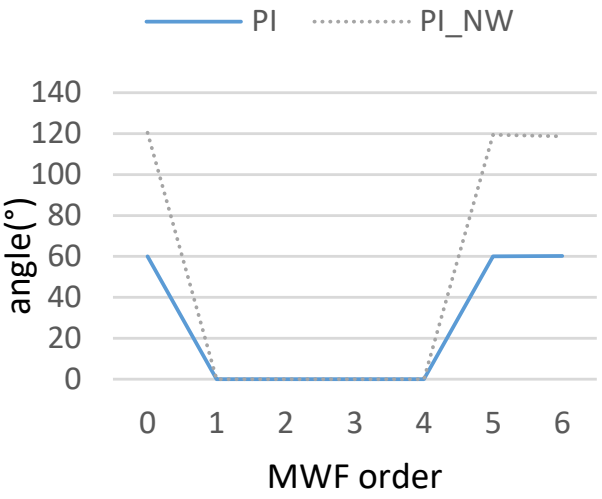

Fig. 4. Relationship between nulling angle and MWF order.

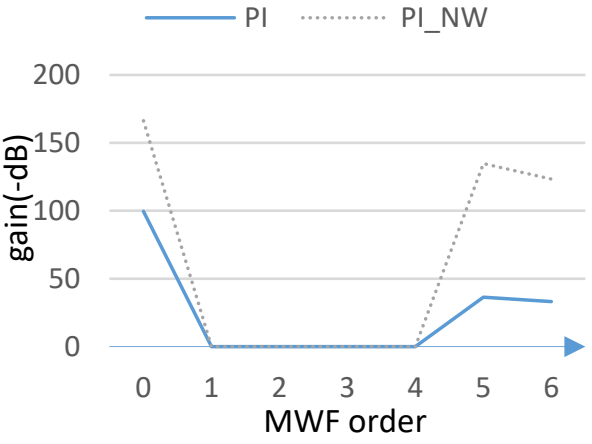

Fig. 5. Relationship between nulling gain and MWF order.

B. MCSA-MWF-LNW-PI algorithm ideal state simulation

The BeiDou data used in this paper consists of seven channels of data, with a total of seven rows, so we chose

to use a seven-element uniform circular array when performing the simulation in the ideal case.

Simulation of the LNWD algorithm and the MCSA-MWF-LNW-PI in a 2D uniform circular-center array. A seven-element circular-center array is set up with a signal-to-noise ratio of -20 dB, a dry-to-noise ratio of 60 dB, a snap count of 2046, a signal incoming direction (10°, 45°), and the incoming direction of the interference is (20°, 50°). The orientation diagram is shown in Fig. 6. The nulling after using the MCSA-MWF of order 6 is basically the same as the ideal case, which can be used in both nulling widen as well as nulling widen and deepening algorithms, which has a very low impact on the nulling but serves to reduce the dimension, which reduces the computational effort.

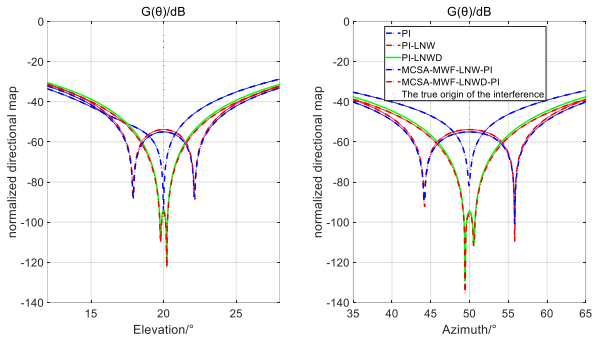

(a) (b)

Fig. 6. Comparison of direction map nulling for MCSA-MWF and ideal algorithm: (a) elevation orientation diagram and (b) azimuth orientation diagram.

C. MCSA-MWF-LNW-PI algorithm simulation of real data

The BeiDou data used in this paper consists of seven channels of data, with a total of seven rows, so we chose to use a seven-element uniform circular array when performing the simulation in the ideal case.

According to the official documents of the BeiDou satellite navigation system, the space constellation of BeiDou-3 consists of three geostationary orbit satellites (GEO), three inclined geosynchronous orbit satellites (IGSO), and 24 medium circular earth orbit satellites (MEO). The LNWD algorithm and the MCSA-MWF-LNWD algorithm simulated for the sampled B3I signal. The B3I signal is sampled with three interfering data of seven channels, with a total of seven rows, and each row represents the data of one channel, and the data time length is about 100 ms. The sampled data is the signal of the BD B3 frequency point, with a data sampling rate of 62 MHz, and an intermediate frequency of 80.52 MHz.

Figure 7 shows the comparison of the antenna gain direction plots after using the PI algorithm in two cases, where PI (blue line) is the ideal case. Its purpose is to see the effect of the nulling widen algorithm using the MCSA-MWF on the nulling. From the two graphs in Fig. 7, it can be seen that the nulling case (i.e., the lowest gain point) of the MCSA-MWF-LNW-PI algorithm is almost the same as the nulling of the ideal case, while the other two algorithms nulling cases are always different from the ideal case. So, it can be concluded that all the nulling cases after using MCSA-MWF with order 6 are basically the same as the ideal case, which can be used for the nulling widen and deepening algorithms, which have less effect on nulling but play the role of dimension reduction, thus reducing the amount of computation.

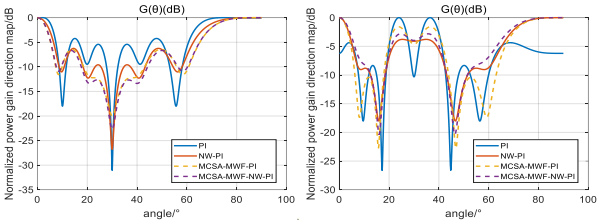

Fig. 7. Comparison of directional map nulling between MCSA-MWF and ideal algorithm under BeiDou data.

V. CONCLUSION

In this paper, we solve the problem of large inverse matrix operation of invalid broadening in adaptive anti-jamming algorithms under high dynamics. The performances of three commonly used MWF algorithms are compared, and the results show that MCSA-MWF greatly reduces the computational volume and dimension compared with CSA-MWF and GRS-MWF. Finally, we chose to combine the MCSA-MWF algorithm with the traditional zeroing and widening method and propose a new MCSA-MWF-LNWD algorithm, which improves the stability when using small snapshot data in real high dynamic environments.

In addition, several simulations including the ideal case of seven-element uniform circular array test and using seven-element real BeiDou data are conducted, and the results show that the nulling using MCSA-MWF is very close to the ideal case. This approach can be effectively applied to both cavitation widening and cavitation deepening algorithms. Although the cavitation effect may be degraded, it plays a key role in dimensionality reduction, which greatly reduces the computational effort. Compared with the computational complexity of the conventional nulling widen class algorithm for direct inverse $O\left(M^3\right)$. The computational complexity of the algorithm based on the MCSA-MWF is $O\left(rM^2\right)$, which greatly reduces the computational complexity.

REFERENCES

[1] J. R. Sklar, "Interference mitigation approaches for the global positioning system," *Lincoln Laboratory Journal*, vol. 14, no. 2, pp. 167-179, 2003.

[2] T. H. Kim, C. S. Sin, S. Lee, and J. H. Kim, "Analysis of performance of GPS L1 signal generator in GPS L1 signal," *IEEE 14th International Conference on Control, Automation and Systems,* pp. 1006-1009, Oct. 2014.

[3] D. C. Ricks, "Efficient architectures for implementing adaptive algorithms," in *Proc. 2000 Antenna Applications Symposium,* Allerton Park, Monticello, IL*,* pp. 29-41, Sep. 2000.

[4] R. J. Mailloux, "Covariance matrix augmentation to produce adaptive array pattern troughs," *IEEE Antennas and Propagation Society International Symposium. Dig.,* vol. 1, 1995.

[5] F. Shen, F. Chen, and J. Song, "Robust adaptive beamforming based on steering vector estimation and covariance matrix reconstruction," *IEEE Commun. Lett.*, vol. 19, no. 9, pp. 1636-1639, 2015.

[6] R. T. Compton, "The power-inversion adaptive array: Concept and performance," *IEEE Trans. Aerosp. Electron. Syst*, vol. 6, pp. 803-814, 1979.

[7] M. Zatman, "Production of adaptive array troughs by dispersion synthesis," *Electronics Lett.*, vol. 31, no. 25, pp. 2141-2142, 1995.

[8] R. Li, Y. Wang, and S. Wan, "Adaptive antenna direction map interference nulling widen method," *Modern Radar*, no. 2, pp. 42-45, 2003.

[9] Y. Cong, D. Feng, and H. Li, "A highly dynamic GNSS anti-jamming algorithm based on nulling widen and deepening," *J. Jilin Univ.: Information Sci. Ed.*, vol. 38, no. 1, pp. 1-8, 2020.

[10] X. Zeng, M. Li, and J. Nie, "Analysis of the effect of platform motion on antenna array performance in satellite navigation systems," *J. National Univ. Defence Technol.,* vol. 33, no. 1, pp. 5-8, 2011.

[11] X. Zeng, "Research on delay, quantisation and motion adaptation techniques in satellite navigation anti-jamming," M.S. thesis, National University of Defence Science and Technology, 2014.

[12] D. Lu, L. Ge, W. Wang, L. Wang, Q. Jia, and R. Wu, "A high-dynamic null-widen algorithm based on reduced-dimension space-time adaptive processing," *J. Electron. Inf. Technol.,* vol. 38, no. 1, pp. 216-221, 2016.

[13] Y. Ma, Y. Xu, and J. Li, "A high-dynamic null-widen GPS anti-jamming algorithm based on statistical model of the changing interference DOA," in *China Satellite Navigation Conference (CSNC) 2014 Proceedings,* Vol. 1, Springer, Berlin Heidelberg, 2014.

[14] R. J. Mailloux, "Covariance matrix augmentation to produce adaptive array pattern troughs," *IEEE Antennas and Propagation Society International Symposium. Dig.,* vol. 1, pp. 1-4, 1995.

[15] J. R. Guerci, "Theory and application of covariance matrix tapers for robust adaptive beamforming," *IEEE Trans. Signal Process.,* vol. 47, no. 3, pp. 977-985, 1999.

[16] M. Zatman and J. R. Guerci, "Comment on theory and application of covariance matrix tapers for robust adaptive beamforming," *IEEE Trans. Signal Process.,* vol. 48, no. 6, pp. 1796-1800, 2000.

[17] M. Rubsamen, C. Gerlach, and A. B. Gershman, "Low-rank covariance matrix tapering for robust adaptive beamforming," in *Proc. 2008 IEEE Int. Conf. Acoustics, Speech and Signal Processing,* Las Vegas, NV, pp. 2333-2336, 2008.

[18] Z. Liu, Z. Su, and Q. Hu, "Robust sidelobes cancellation algorithm with null widen," *J. Electron. Inf. Technol.,* vol. 38, no. 5, pp. 565-570, 2016.

[19] X. Yang, S. Li, T. Long, and T. K. Sarkar, "Adaptive null widen method in wideband beamforming for rapidly moving interference suppression," *Electron. Lett.,* vol. 54, no. 11, pp. 1003-1005, 2018.

[20] W. Li and B. Yang, "An improved null widen beamforming method based on covariance matrix reconstruction," in *2017 International Applied Computational Electromagnetics Society Symposium-Italy (ACES). IEEE,* Firenze, Italy, pp. 1-2, 2017.

[21] J. Yang, J. Lu, X. Liu, and G. Liao, "Robust null widen beamforming based on covariance matrix reconstruction via virtual interference sources," *Sensors,* vol. 20, no. 1865, 2020.

[22] J. Qian, Z. He, and J. Xie, "Null widen adaptive beamforming based on covariance matrix reconstruction and similarity constraint," *EURASIP J. Adv. Signal Process.,* vol. 2017, 2017.

[23] Z. Liu, S. Zhao, and G. Zhang, "Robust adaptive beamforming for sidelobe canceller with null widening," *IEEE Sensors Journal,* vol. 19, no. 23, pp. 11213-11220, 2019.

[24] J. S. Goldstein, I. S. Reed, and L. L. Scharf, "A multistage representation of the Wiener filter based on orthogonal projections," *IEEE Trans. Inf. Theory*, vol. 44, no. 7, pp. 2943-2959, Nov. 1998.

[25] D. C. Ricks and J. S. Goldstein, "Efficient architectures for implementing adaptive algorithms," in *Proc. 2000 Antenna Applications Symposium,* Allerton Park, Monticello, IL, pp. 29-41, Sep. 2000.

[26] D. C. Ricks, P. G. Cifuentes, and J. S. Goldstein, "Adaptive beamforming using multistage Wiener filter with a soft stop," *Conference Record of the Thirty-Fifth Asilomar Conference on Signals,*

Systems and Computers, Pacific Grove, CA, pp. 1401-1406, Nov. 2001.

[27] L. Huang, J. Zhang, X. Xu, and Z. Ye, "Robust adaptive beamforming with a novel interference-plus-noise covariance matrix reconstruction method," *IEEE Trans. Signal Process.,* vol. 63, no. 7, pp. 1643-1650, Apr. 2015.

[28] J. R. Guerci, "Theory and application of covariance matrix tapers for robust adaptive beamforming," *IEEE Trans. Signal Process.,* vol. 47, no. 4, pp. 977-985, Apr. 1999.

[29] Q. Ding, Y. Wang, and Y. Zhang, "An efficient implementation algorithm for multilevel Wiener filter in adaptive arrays," *Journal of Electronics and Information,* vol. 28, no. 5, pp. 936-940, 2006.

[30] BeiDou satellite navigation system space signal interface specification part 4: open service signal B3I, 2020.

[31] Q. Ding, Y. Wang, and Y. Zhang, "An efficient implementation algorithm for multilevel Wiener filter in adaptive arrays," *Journal of Electronics and Information,* vol. 28, no. 5, pp. 936-940, 2006.

[32] X. Wang and T. Li, "A zero-sag spreading and deepening algorithm for arbitrary planar arrays," *Journal of Terahertz Science and Electronic Information,* vol. 20, no. 8, pp. 830-835, 2022.

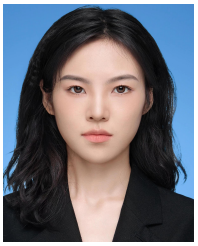

Xiao Li received the B.S. degree in Remote Sensing Science and Technology from the School of Electrical Engineering, Xidian University in 2023. She is now pursuing her master's degree in the Department of Electromagnetic Field and Microwave Technology at the same university. Her current research interests include smart antenna immunity.

Xinhuai Wang received the B.E. degree in electronic science and technology and Ph.D. degree in radio physics from Xidian University, Xi'an, China, in 2004 and 2010, respectively. Since 2010, he has been with the National Key Laboratory of Antennas and Microwave Technology, Xidian University, as a Lecturer. He has been an Associate Professor with Xidian University since 2014. He has been a Professor and Doctoral Supervisor since 2020. His recent research interests are mainly in microwave circuits and smart antenna system design.